Published in final edited form as:
Circulation. 2007 November 13; 116(20): 2260–2268. doi:10.1161/CIRCULATIONAHA.107.703330.

Mutation in Glycerol-3-Phosphate Dehydrogenase 1–Like Gene (*GPD1-L*) Decreases Cardiac Na^+ Current and Causes Inherited Arrhythmias

Barry London, MD, PhD, **Michael Michalec, MS**, **Haider Mehdi, PhD**, **Xiaodong Zhu, PhD**, **Laurie Kerchner, BS**, **Shamarendra Sanyal, PhD**, **Prakash C. Viswanathan, PhD**, **Arnold E. Pfahnl, MD, PhD**, **Lijuan L. Shang, PhD**, **Mohan Madhusudanan, MD**, **Catherine J. Baty, PhD**, **Stephen Lagana, BA**, **Ryan Aleong, MD**, **Rebecca Gutmann, RN, BSN**, **Michael J. Ackerman, MD, PhD**, **Dennis M. McNamara, MD**, **Raul Weiss, MD**, and **Samuel C. Dudley Jr, MD, PhD**

Cardiovascular Institute (B.L., M. Michalec, H.M., X.Z., L.K., P.C.V., M. Madhusadanan, S.L., R.A., R.G., D.M.M.) and Department of Cell Biology and Physiology (B.L., P.C.V., C.J.B.), University of Pittsburgh, Pittsburgh Pa; Department of Cardiology, Emory University and Atlanta VA, Medical Center, Atlanta, Ga (S.S., A.E.P., L.L.S., S.C.D.); Division of Cardiology, Mayo Clinic College of Medicine, Rochester, Minn (M.J.A.); and Division of Cardiology, Ohio State University, Columbus (R.W.)

Abstract

Background—Brugada syndrome is a rare, autosomal-dominant, male-predominant form of idiopathic ventricular fibrillation characterized by a right bundle-branch block and ST elevation in the right precordial leads of the surface ECG. Mutations in the cardiac Na^+ channel SCN5A on chromosome 3p21 cause ≈20% of the cases of Brugada syndrome; most mutations decrease inward Na^+ current, some by preventing trafficking of the channels to the surface membrane. We previously used positional cloning to identify a new locus on chromosome 3p24 in a large family with Brugada syndrome and excluded *SCN5A* as a candidate gene.

Methods and Results—We used direct sequencing to identify a mutation (A280V) in a conserved amino acid of the glycerol-3-phosphate dehydrogenase 1–like (*GPD1-L*) gene. The mutation was present in all affected individuals and absent in >500 control subjects. GPD1-L RNA and protein are abundant in the heart. Compared with wild-type GPD1-L, coexpression of A280V GPD1-L with SCN5A in HEK cells reduced inward Na^+ currents by ≈50% ($P<0.005$). Wild-type GPD1-L localized near the cell surface to a greater extent than A280V GPD1-L. Coexpression of A280V GPD1-L with SCN5A reduced SCN5A cell surface expression by 31±5% ($P=0.01$).

Conclusions—*GPD1-L* is a novel gene that may affect trafficking of the cardiac Na^+ channel to the cell surface. A GPD1-L mutation decreases SCN5A surface membrane expression, reduces inward Na^+ current, and causes Brugada syndrome.

Keywords

arrhythmia; electrophysiology; genetics; ion channels; sodium

Correspondence to Barry London, MD, PhD, Cardiovascular Institute, University of Pittsburgh Medical Center, Scaife S-572, 200 Lothrop St, Pittsburgh, PA 15213–2582. londonb@upmc.edu.

Disclosures
None.

Brugada syndrome is a rare, autosomal-dominant, male-predominant form of idiopathic ventricular fibrillation characterized by a right bundle-branch block and ST elevation in the right precordial leads of the surface ECG.[1–4] Affected individuals develop syncope, ventricular arrhythmias, and sudden death, and the only proven therapy for patients at high risk is an implanted cardioverter-defibrillator (ICD). More than 80 mutations of the cardiac Na^+ channel SCN5A on chromosome 3p21 cause ≈20% of the cases of Brugada syndrome.[1,5,6] Most of the known SCN5A mutations responsible for Brugada syndrome decrease inward Na^+ current (I_{Na}), some by preventing trafficking of channels to the surface membrane.[7–10] Na^+ channel blockers are clinically useful because they enhance the ECG phenotype.[11] More recently, mutations in the cardiac Ca^{2+} channel CACNA1c ($Ca_v1.2$) and its β-subunit CACNB2b that decrease inward Ca^{2+} current have been shown to cause an overlap syndrome with both a short-QT interval and a Brugada syndrome ECG.[12] These findings support the hypothesis that inadequate depolarizing current in the epicardium of the right ventricle, where the transient outward repolarizing current is greatest, causes premature repolarization, current flow and ST elevation on the ECG, phase II reentry, and arrhythmias.[13] To date, only ion channel–related genes have been shown to cause Brugada syndrome.

We previously linked a large multigenerational family of Italian descent with Brugada syndrome (family FN; Figure 1) to a locus at chromosome 3p22–24 with a LOD (logarithm of odds) score >4.0 and excluded *SCN5A* as a candidate by linkage and direct sequencing.[14] We now report the identification of the gene and the mutation responsible for Brugada syndrome in this family.

Methods

Clinical Testing

The Institutional Review Board at the University of Pittsburgh approved all human studies. The proband and his family were referred to our institution; the clinical characteristics of the family have been reported previously.[14] Clinical follow-up of the family has continued for the last 10 years, including enrollment of new individuals and ECGs on at-risk individuals every 6 months. To date, ICDs have been placed in 4 genotypically affected individuals on the basis of clinical criteria. The proband had 2 episodes of polymorphic ventricular tachycardia terminated by appropriate ICD shocks,[14] and 1 affected brother of the proband had a 20-beat episode of ventricular flutter (rate, ≈300 bpm) that self-terminated and did not require an ICD shock.

Identification and Sequencing *GPD1-L*

Selected candidate genes and *GPD1-L* were sequenced with BigDye Terminator version 1.1 (Applied Biosystems, catalog No. 4337450, Foster City, Calif). Sequencing reactions were analyzed on the ABI 310 Genetic Analyzer (Applied Biosystems) using sequencing analysis software and BLAST. The following oligonucleotides were designed and used for polymerase chain reaction amplification and sequencing of *GPD1-L*: exon 1f, CACGGTCCAGGCGGCTACATTC; exon 1R, TGCTCGAGCCTCCACCAAGTCCTT; exon 2F, GTTTATGTTTTTCTTTTCCACGAT; exon 2R, AGCAACATAATAGGAAACCCATT exon 3F; CAGGCAAGGTTGATATAAGAGGA; exon 3R, CGAAAAACCGCCACAACTT; exon 4F, AGTTGTGTAGCCATGGGACATCT; exon 4R, TGTTAAGAGGGACAGGGAAGAGTC; exon, 5F, AGGCTGTTATTAATATCCTTGTTG; exon 5R, CCTTGCTTGATGAACTCCTC; exon 6F, CTGTAACGGCATCTGGGCTTTGTC; exon 6R, CAGTTCACCCCAAGCCAGGAGTC; exon 7F, GGCTTCCAGCAGGGGACTGAA; exon

7R, TTATCTGGTCTCATGGGCGACTGA; exon 8F, ACCTGCAATCTGTTAGGACA; and exon 8R, CCGTGATGAGATTACAGTCAA.

Genotyping Family Members and Normal Control Subjects

The C/T base-pair change at position 899 of GPD1-L created an Hyp188I restriction site that was used to screen the entire family and >200 individuals of mixed racial backgrounds from the Pittsburgh area (including ≈100 individuals of Italian descent). In addition, DNA from 300 reference individuals (100 black, 200 white; Coriell Institute, Camden, NJ) was screened by WAVE denaturing high-pressure liquid chromatography (Transgenomic, Inc, Omaha, Neb). Thus, a total of >1000 ethnically diverse reference alleles were screened. Individuals carrying the mutation were confirmed by direct sequencing.

GPD1-L Clones

A full-length human GPD1-L clone in pBS was obtained (identification No. 4820730, Invitrogen, Carlsbad, Calif), and the coding region was subcloned into pBKCMV (Stratagene, La Jolla, Calif) for expression studies and electrophysiology. The A280V mutant was engineered with QuikChange (Stratagene). Adeno-associated viral constructs carrying wild-type (WT) and A280V GPD1-L were generated by insertion of the WT and mutant GPD1-L coding regions between the cytomegalovirus promoter and poly-A trails of double-stranded AAV constructs.

We designed green fluorescent protein (GFP)–fused GPD1-L constructs (WT or A280V) to trace the trafficking of GPD1-L in transiently transfected HEK 293 or COS-7 cells. Briefly, polymerase chain reaction–amplified GPD1-L cDNA was cloned in CT-GFP-TOPO-TA vector (Invitrogen). GPD1-L–GFP fusion constructs (GFP at the C terminus) were identified by DNA sequencing and Western blotting of cell lysates of transiently transfected COS-7 cells in which GFP-fused GPD1-L ran as a slower band (≈70 kDa) compared with the GPD1-L band (≈40 kDa).

Cell Culture

HEK 293 and COS-7 cells were maintained in Dulbecco's modified Eagle's medium supplemented with 10% FBS (Invitrogen:Gibco–BRL Life Technologies, Carlsbad, Calif), 100 $U \cdot mL^{-1}$ penicillin, and 100 $\mu g \cdot mL^{-1}$ streptomycin at 37°C in CO_2-controlled environments. The HEK cell line constitutively expressing SCN5A was generated by transfection with an SCN5A IRES-GFP construct, isolation and expansion of GFP-positive cells, and maintenance in the above medium plus G418 (Geneticin reagent, Invitrogen) 0.2 mg/mL at 37°C in CO_2-controlled environments. HEK 293 or COS-7 cells were transfected by the standard calcium phosphate method or lipofectamine 2000 (Invitrogen) using the manufacturer's protocol. The AAV–GPD1-L stocks were produced by the adenovirus-free, triple-plasmid cotransfection method, and cells were infected by standard methods.

Tissue and Cellular Expression of GPD1-L

Analysis of the expression of GPD1-L mRNA was performed by Northern blot. Polymerase chain reaction using the human GPD1-L cDNA as a template and the following primers produced a 345-bp fragment specific for human GPD1-L mRNA: GPD1-LF, CTCCAAGGACCGCAGACTT; and GPD1-LR, ACTGCCCAGTACATCTTTGCTAAT. Polymerase chain reaction product (10 ng) was labeled with [α^{32}P]-dCTP using the Redi-prime II kit (Amersham, catalog No. RPN1633, Piscataway, NJ) and hybridized to a multiple human tissue Northern blot (Clontech, Mountain View, Calif) using the specified protocol for Northern blotting.

Western blotting was performed using standard protocols. For membrane proteins, mouse or human hearts were pulverized under liquid nitrogen and homogenized with a Tissuemiser (Fisher Scientific, Waltham, Mass). The homogenate was centrifuged at 1000*g* for 10 minutes at 4°C; the supernatant was spun at 100 000*g* for 1 hour at 4°C; and the pellet was resuspended in a buffer containing 1% SDS and then centrifuged at 10 000*g* for 10 minutes at 4°C to remove the insoluble fraction. For total protein, hearts were pulverized and homogenized as above, whereas cells were disrupted by sonication. For both cells and hearts, the insoluble fraction was removed by centrifugation at 15 000*g* for 10 minutes at 4°C.

Protein concentrations were determined (BioRad Protein Assay, BioRad Laboratories, Hercules, Calif), and 10 to 30 μg protein per lane was used for the Western analysis. SDS-PAGE was carried out with 4% to 15% gradient polyacrylamide gels (BioRad Laboratories) and polyvinylidene difluoride membrane (Immobilon-P, Bedford, Mass). The primary antibody was directed against the peptide sequence QTSAEVYRILRQKGLLDK corresponding to amino acids 303 through 320 in mouse GPD1-L protein (accession number NP_780589) and was prepared in rabbits and chickens by Zymed Laboratories (San Francisco, Calif). The chosen peptide was highly conserved in human GPD1-L, in which the corresponding sequence is QTSAEVYRILKQKGLLDK (accession number NM_015141). This antibody was diluted 1:1000 in 5% nonfat dried milk (Carnation, Solon, Ohio) in Tris-buffered saline (TBS; 10 mmol/L Tris, 150 mmol/L NaCl, ph 7.4), and immunoblots were incubated overnight at 4°C. After washes in TBS with 0.05% Tween 20, blots were incubated for 1 hour at room temperature with alkaline phosphatase–conjugated goat anti-rabbit IgG secondary antibody (Jackson ImmunoResearch, West Grove, Pa) diluted 1:7500 in nonfat dried milk, washed in TBS with 0.05% Tween 20, incubated in the chemiluminescent substrate reagent CDP-Star (Boehringer Mannheim, Indianapolis, Ind), and exposed to Kodak BioMax-MR film for signal detection.

Whole-Cell Voltage-Clamp Electrophysiology

The recombinant Nav1.4 (SCN4A) and Nav1.5 (SCN5A) Na^+ channels were subcloned in the expression vector pCGI (GFPIres) for bicistronic expression of the channel protein and a GFP reporter. SCN5A was provided by David C. Johns, Bradley H. Nuss, and Eduardo Marban (Johns Hopkins University), and SCN4A was provided by Jeffrey R. Balser and Al George (Vanderbilt University, Nashville, Tenn). cDNAs of Nav1.5 or Nav1.4 and GPD1-L (WT or A280V) were transiently cotransfected into HEK-293 cells using lipofectamine 2000 (Invitrogen). The cells were cultured in Dulbecco's modified Eagle's medium supplemented with 10% FBS, 100 $U \cdot mL^{-1}$ penicillin and 100 $\mu g \cdot mL^{-1}$ streptomycin in a 5% CO_2 incubator at 37°C for 1 to 4 days.

Whole-cell Na^+ currents were recorded from cells expressing GFP at room temperature (Axopatch 200B, Axon Instruments, Foster City, Calif). Electrodes of 1 to 2 mol/LΩ were filled with a pipette solution containing (in mmol/L) NaF 10, CsF 110, CsCl 20, EGTA 10, and HEPES 10 (pH 7.35 with CsOH). The bath solution contained (in mmol/L) NaCl 145, KCl 4.5, $CaCl_2$ 1.5, $MgCl_2$ 1, and HEPES 10 (titrated to pH 7.35 with CsOH). In all recordings, the potentials were corrected for the liquid junction, and 80% of the series resistance was compensated, yielding a maximum voltage error of ≈1 mV. Na^+ currents (I_{Na}) were sampled at 20 kHz through an analog-to-digital converter (DigiData 1200, Molecular Devices, Sunnyvale, Calif) and low-pass filtered at 5 kHz. Na^+ channel data were collected and analyzed with pClamp 9.2 software (Molecular Devices). Cell capacitance was recorded directly from the Axopatch 200B amplifier after nullifying the transients following patch rupture. Relatively small cells were used to ensure better voltage control. To minimize time-dependent drift in gating parameters, all protocols were initiated 5 minutes after whole-cell configuration was obtained.

Intermediate inactivation was assessed with a 2-pulse protocol. The first pulse to −20 mV from a holding potential of −120 mV ranged from 1 to 1000 ms in duration to ensure that channels entered the intermediate inactivation state. This was followed by a brief recovery period to −120 mV for 20 ms to allow recovery from fast inactivation. The peak current during the second test pulse to −20 mV was normalized to the first pulse, and the points were fit using a single exponential function. Fast inactivation was assessed during voltage depolarizations from a holding potential of −120 mV to −30, −20, −10, and 0 mV. Current decay was best fit using a 2-exponential function, and values of τ_{fast} and τ_{slow} were determined. Recovery from inactivation (after a 1000-ms depolarization to −20 mV from a holding potential of −120 mV) was fit using a 2-exponential function, with τ_{fast} representing recovery from fast inactivation and τ_{slow} representing recovery from slow inactivation.

Intracellular Expression of GPD1-L and SCN5A

SCN5A was cloned into pRcCMV (Invitrogen) for immunofluorescence studies. For confocal fluorescence microscopy, 24-hour-posttransfected COS-7 or HEK 293 cells with GPD1-L–GFP constructs (WT or A280V) were fixed in 2% paraformaldehyde in PBS and mounted on glass slides. For immunofluorescence, 2-day-posttransfected HEK 293 cells were fixed in 2% paraformaldehyde in PBS, made permeable with 0.1% Triton-X in PBS, and blocked with 2% BSA in PBS. Cells cotransfected with GPD1-L–GFP and SCN5A were incubated for 1 hour at room temperature with rabbit anti-SCN5A from Alomone Labs (Jerusalem, Israel) diluted 1:1000 in 0.5% BSA, washed with 0.5% BSA in PBS to remove unbound primary antibody, and incubated with Cy3-conjugated goat anti-rabbit IgG (Jackson Immunoresearch, West Grove, Pa) and phalloidin Cy5 in some experiments to delineate cortical actin.

Imaging and Quantitative Immunofluorescence

Cells were imaged with a Leica TCS-SL confocal microscope and captured with Leica confocal software (Leica Microsystems, Mannheim, Germany). For each confocal series, the image that showed the best cell surface membrane staining was selected for quantitative immunofluorescence. To determine the proportion of SCN5A expression in or near the membrane, entire cell fluorescence and membrane regions were delineated with Metamorph computer software (Molecular Devices). Each cell was outlined; the inner aspect of the cell membrane was outlined; and the number of pixels in the cell with and without the membrane region was determined. The difference between these 2 readings divided by the total number of pixels in the entire cell was calculated to determine the percent of total SCN5A in the cell that localized near the cell surface. In addition, the proportion of the cell designated surface membrane was determined for each group.

Biotinylation of Cell Surface SCN5A

Biotinylation of cell surface proteins was performed with the Pinpoint Cell Surface Protein Isolation Kit (Pierce, Rockford, Ill). Briefly, HEK 293 cells constitutively expressing SCN5A were infected with adeno-associated virus carrying WT or A280V GPD1-L. After 2 days, cells were washed with PBS and incubated with Sulfo-NHS-SS-Biotin for 30 minutes at 4°C. The reaction was quenched, and cells were gently removed from the flask, placed in a conical tube, washed in TBS, and divided into pellets at 500*g*. Cell pellets were sonicated in lysis buffer with protease inhibitors, and the cell lysate was centrifuged at 10 000*g* for 2 minutes at 4°C. Biotinylated proteins were isolated on a column containing immobilized NeutrAvidin protein (Pierce Biotechnology, Inc, Rockford, Ill). After washes, surface proteins were eluted with SDS-PAGE sample buffer containing 50 mmol/L dithiothreitol and electrophoresed for subsequent Western blotting as described above. For detection of SCN5A, primary antibody (described above) was diluted 1:1000.

Radiographs were scanned and digitized for analysis using Quantity One quantification software (BioRad Laboratories). Bands of interest were delineated, and densitometries were calculated on the basis of the number of pixels. Total protein was normalized to Coomassie stains to account for differences in loading, and membrane SCN5A/total SCN5A was compared for cells infected with AAV-A280V versus AAV-WT GPD1-L.

Statistical Analysis

Data are presented as mean±SEM. Significance was determined using 2-tailed Student *t* test for paired or unpaired variables, and ANOVA (Microcal Origin, Northampton, Mass) was used for continuous variables. A value of $P<0.05$ was considered significant.

The authors had full access to and take full responsibility for the integrity of the data. All authors have read and agree to the manuscript as written.

Results

A Mutation in GPD1-L Causes Brugada Syndrome

The region of linkage in the FN family was narrowed to ≈1 million bp on chromosome 3p24 by fine mapping, and an electronic contig was generated. The candidate genes *KCNH8* (Elk1 K^+ channel), *DNLC1* (dynein cytoplasmic light-intermediate peptide 1), *TGFB2* (tissue growth factor-β2), and *PDLC1* (phospholipase C) were eliminated by single-strand conformational polymorphism and/or direct sequencing. RNA from 2 putative genes with no known function within the linkage region was detected in the heart using reverse-transcription polymerase chain reaction; direct sequencing identified no mutations in *C3ORF3* (KIAA1173) and a C/T base-pair change (C899T) in *GPD1-L* (KIAA0089, NM_015141) leading to an alanine-to-valine substitution at amino acid 280 (A280V) in exon 6 (Figure 2A). All 16 phenotypically affected individuals and 27 others in the FN family carried the A280V mutation (37% penetrance; Figure 1). All of the other mutation carriers >18 years of age had been previously classified as phenotypically uncertain because of QRS prolongation and/or ST segment or J-point elevation. The 280V allele was not identified in >1000 reference alleles from individuals of mixed racial background. No mutations in *GPD1-L* were identified in the probands of 19 smaller families with Brugada syndrome.

The human GPD1-L mRNA is 3954 bp long and encodes a protein predicted to be 351 amino acids in length. There is 84% homology with the GPD protein, a dimer involved in the glycerol phosphate shuttle that transfers electrons from cytosolic NADH to the mitochondrial transport chain and may play roles in energy production, osmoregulation, tumor growth, and apoptosis.[15] The alanine at position 280 is conserved in all higher organisms for which sequence exists, including human, orangutan, mouse, rat, dog, cow, pig, and salmon for GPD1-L and human, mouse, rat, dog, and cod for GPD. The putative NAD^+ binding site and the catalytic site in GPD are conserved in GPD1-L (Figure 2A).

GPD1-L Is Expressed in the Heart

GPD1-L mRNA is most highly expressed in heart tissue, with lower levels in the skeletal muscle, kidney, lung, and other organs (Figure 2B). GPD1-L protein is present in homogenates from mouse and human heart and is concentrated in the membrane fraction (Figure 2C and 2D). GPD1-L protein is present in similar abundance in male compared with female rabbit hearts and in right compared with left ventricles (data not shown).

A280V GPD1-L Decreases Inward SCN5A Na^+ Current

WT or A280V GPD1-L and SCN5A were transiently cotransfected into HEK cells (Figure 3A and 3B). Overexpression of WT GPD1-L did not significantly affect the amplitude of I_{Na}, but overexpression of A280V GPD1-L decreased I_{Na} by 48% (at −20 mV, from −570 to −298 pA/pF; *P*=0.004) compared with WT GPD1-L. Similar results were obtained using transient transfections of WT or A280V GPD1-L into an HEK cell line stably expressing SCN5A (data not shown).

The A280V mutation did not cause any significant changes in the activation or inactivation kinetics of I_{Na} (Figure 3C). The steady-state inactivation curves were fit using a Boltzmann function, and the $V_{1/2}$ and k (slope factor) were −95.2±0.7 mV and 6.1±0.1 for mock-transfected cells (n=11), −93.9±1.5 mV and 5.8±0.1 for cells transfected with WT GPD1-L (n=15), and −94.9±1.6 mV and 6.4±0.3 for cells transfected with A280V GPD1-L (n=16; *P*=NS). Similarly, the $V_{1/2}$ and k for activation were −41.0±0.8 mV and 7.3±0.3 for mock-transfected cells (n=11), −41.5±0.9 mV and 6.6±0.2 for cells transfected with WT GPD1-L (n=15), and −39.2±1.2 mV and 7.2±0.3 for cells transfected with A280V GPD1-L (n=16; *P*=NS). In addition, the A280V mutation did not alter the time course of the development of or recovery from inactivation. The time constants for the development of intermediate inactivation, assessed using a 2-pulse protocol, were 254±42 ms for cells transfected with WT GPD1-L (n=11) and 222±41 ms for cells transfected with A280V GPD1-L (n=13; *P*=NS). The time constants for fast inactivation, determined using the fit to a 2-exponential function during voltage steps from −120 mV to between −30 and 0 mV, also were unaffected. At −20 mV, τ_{fast}=0.95±0.05 ms and τ_{slow}=5.68±0.42 ms for cells transfected with WT GPD1-L (n=15), and τ_{fast}=1.05±0.08 ms and τ_{slow}=6.59±0.85 ms for cells transfected with A280V GPD1-L (n=16; *P*=NS). Finally, the time constants for recovery from inactivation were unaffected, with τ_{fast}=13.5±1.5 ms and τ_{slow}=133±15 ms for cells transfected with WT GPD1-L (n=7) and τ_{fast}=16.8±3.7 ms and τ_{slow}=179±33 ms for cells transfected with A280V GPD1-L (n=8; *P*=NS).

The effect of the GPD1-L mutation on current amplitude was specific for the cardiac channel isoform. Cotransfection of A280V GPD1-L with the skeletal muscle Na^+ channel SCN4A, which differs considerably in the intracellular linkers between domains I to II and domains II to III, did not affect the Na^+ current (Figure 3D). A280V GPD1-L also did not alter currents from the K^+ channel HERG (data not shown).

Intracellular Localization of GPD1-L Is Affected by the A280V Mutation

On the basis of its enrichment in membrane preparations (Figure 2C), a hydrophobicity analysis that suggested the presence of a transmembrane domain at the N terminus, and data suggesting that GPD binds to the membrane by an amphipathic α helix,[16] we hypothesized that GPD1-L is most likely a membrane-associated protein. We therefore engineered fusion proteins with GFP attached to the C terminus of WT and A280V GPD1-L. Confocal microscopy of transfected COS-7 cells (Figure 4A and 4B) and HEK 293 cells (Figure 4C and 4D) showed that WT GPD1-L–GFP localized to the region of the plasma membrane to a greater extent than A280V GPD1-L–GFP. Similar results were found using immunostaining of untagged WT and A280V GPD1-L (data not shown).

Surface Expression of SCN5A Is Decreased by the A280V GPD1-L Mutation

Expression of SCN5A near the surface membrane, measured by immunostaining and confocal microscopy, was decreased by 48% in HEK cells cotransfected with SCN5A and A280V GPD1-L compared with WT GPD1-L (n=16 each; *P*=0.01; Figure 5A and 5B). Biotinylation of membrane proteins (Figure 5C) confirmed the decreased surface expression of SCN5A in cells infected with AAV-A280V GPD1-L compared with AAV-WT GPD1-L

(31±5%; n=5; *P*=0.01), with no difference in total SCN5A protein. Of note, GPD1-L was not detected on the outer surface of the plasma membrane, although this could reflect a limited number of accessible lysine residues and/or steric hindrance to biotinylation.

Biotinylation experiments (Figure 5C) and coimmunoprecipitation of protein preparations from GPD1-L–transfected HEK cells stably expressing SCN5A and mouse hearts (data not shown) failed to show direct interactions between GPD1-L and SCN5A. Thus, without overt binding of GPD1-L to SCN5A, the A280V GPD1-L mutation interferes with intracellular localization of the mutant GPD1-L and decreases surface expression of SCN5A, leading to a decrease in I_{Na} and to Brugada syndrome.

Discussion

Arrhythmias remain a major health problem, leading to >250 000 sudden deaths in the United States each year.[17] After the initial identification of the K^+ and Na^+ channel genes responsible for the long-QT syndrome by positional cloning and candidate positional cloning at the LQT loci, mutations in ion channel genes also were identified in patients with short-QT syndrome, Brugada syndrome, inherited conduction defects, inherited atrial fibrillation, and catecholaminergic ventricular tachycardia, predominantly using a candidate gene approach.[18,19] A great deal has been learned from the ion channel mutations that cause these rare inherited arrhythmopathies. Mutations in genes other than ion channels are less common causes of inherited arrhythmias. One example is ankyrin-B, a membrane adaptor protein that acts as an ion channel scaffold and was identified as the gene responsible for the LQT4 form of long-QT syndrome in a large family.[20] Here, we used positional cloning to identify a novel gene not previously known to be important for cardiac electrophysiology or arrhythmias.

Ion channel defects have been identified as a cause of sudden infant death syndrome,[21] and Van Norstrand et al[22] recently identified 3 mutations in *GPD1-L* in necropsy tissue from infants with autopsy-negative sudden unexplained death. The family we describe has conduction disease that progresses with age.[14] Age dependency of conduction disease is well described for SCN5A mutations in both humans and gene-targeted mice.[23,24] GPD1-L mutations, which also affect I_{Na}, may lead to progressive conduction disease and the age dependency of the ECG phenotype in this family by a similar mechanism. Thus, although *GPD1-L* does not appear to be a common cause of Brugada syndrome on the basis of work by our group and others,[25] it is a candidate gene for other syndromes associated with Na^+ channel defects and arrhythmias. In addition, determining the mechanisms by which GPD1-L affects Na^+ current may elucidate additional genes responsible for Brugada syndrome and other inherited arrhythmia syndromes.

The GPD1-L mutation may cause Brugada syndrome by reducing Na^+ channel trafficking to the plasma membrane. Mutations in SCN5A that affect trafficking can cause Brugada syndrome.[7–10] GPD1-L does not appear to directly associate with SCN5A, but the A280V mutation affects SCN5A surface membrane protein density and the number of functional channels. The mechanism by which GPD1-L mutations alter Na^+ channel membrane expression is currently unknown. There is evidence that oxidative state may affect ion channels and cardiac arrhythmias such as atrial fibrillation.[26,27] On the basis of its homology with GPD, GPD1-L could potentially alter cellular NAD^+/NADH levels and act as a bridge between the metabolic state of the heart and cellular electrophysiology. If true, this could provide a novel explanation for the day-to-day variability in the ECG pattern seen in patients with Brugada syndrome.[1]

Most arrhythmias and sudden cardiac death occur in the setting of ischemia secondary to coronary artery disease or after myocardial damage caused by infarction, viral infection, valve disease, and genetic defects.[28] Although ion channels are critical for the maintenance of normal cardiac rhythm, the mechanisms that lead to the initiation and maintenance of reentrant arrhythmias and their degeneration into fibrillation are only partially understood. Similarly, pharmacological treatments for arrhythmia have not proved to be successful,[29] and the use of ICDs is limited by patient acceptance, decreased quality of life, and cost. The identification of novel arrhythmia genes such as *GPD1-L* may enhance our understanding of the mechanisms of sudden cardiac death and provide novel therapeutic targets.

CLINICAL PERSPECTIVE

Arrhythmias from rare inherited conditions are increasingly recognized as causes of sudden death in otherwise young, healthy subjects. These arrhythmopathies include long-QT syndrome, characterized by QT prolongation on the surface ECG, and Brugada syndrome, characterized by a right bundle-branch block and ST segment elevation in the right precordial leads of the ECG. Most of the genetic mutations identified in these disorders are in ion channels, and clinical screening for genetic defects in cardiac potassium (KvLQT1, HERG, minK, MiRP1) and sodium (SCN5A) channels is currently commercially available (Familion, PGxHealth, New Haven, Conn). We now show that a mutation in a gene with no previously known function, glycerol-3-phosphate dehydrogenase 1–like (*GPD1-L*), causes Brugada syndrome and conduction system disease in a large multigenerational family. Although GPD1-L is not an ion channel itself, the mutation alters trafficking of the cardiac sodium channel SCN5A to the surface membrane and decreases sodium currents. The identification of novel arrhythmia genes such as *GPD1-L* will make presymptomatic diagnosis possible in individuals from families with known mutations and will increase the likelihood of success of genetic screening of subjects with unexplained or inherited arrhythmia syndromes. In addition, these genes may provide novel insights into cellular mechanisms that predispose to the more common arrhythmias that accompany myocardial infarctions and cardiomyopathies.

Acknowledgments

SCN5A was provided by David C. Johns, Bradley H. Nuss, and Eduardo Marban (Johns Hopkins University), and SCN4A was provided by Jeffrey R. Balser and Al George (Vanderbilt University).

Sources of Funding

This study was supported in part by National Institutes of Health National Heart, Lung, and Blood Institute grants R01 HL62300 (Dr London) and R01 HL73753 (Dr Dudley), a US Department of Veterans Affairs Merit Grant (Dr Dudley), and American Heart Association Established Investigator awards (Dr London and Dr Dudley).

References

1. Antzelevitch C, Brugada P, Borggrefe M, Brugada J, Brugada R, Corrado D, Gussak I, LeMarec H, Nademanee K, Perez Riera AR, Shimizu W, Schulze-Bahr E, Tan H, Wilde A. Brugada syndrome: report of the Second Consensus Conference: endorsed by the Heart Rhythm Society and the European Heart Rhythm Association. Circulation. 2005; 111:659–670. [PubMed: 15655131]
2. Brugada J, Brugada P. Further characterization of the syndrome of right bundle branch block, ST segment elevation, and sudden cardiac death. J Cardiovasc Electrophysiol. 1997; 8:325–331. [PubMed: 9083883]
3. Brugada P, Brugada J. Right bundle branch block, persistent ST segment elevation and sudden cardiac death: a distinct clinical and electrocardiographic syndrome: a multicenter report. J Am Coll Cardiol. 1992; 20:1391–1396. [PubMed: 1309182]

4. Grant AO. Electrophysiological basis and genetics of Brugada syndrome. J Cardiovasc Electrophysiol. 2005; 16:S3–S7. [PubMed: 16138883]

5. Chen Q, Kirsch GE, Zhang D, Brugada R, Brugada J, Brugada P, Potenza D, Moya A, Borggrefe M, Breithardt G, Ortiz-Lopez R, Wang Z, Antzelevitch C, O'Brien RE, Schulze-Bahr E, Keating MT, Towbin JA, Wang Q. Genetic basis and molecular mechanism for idiopathic ventricular fibrillation. Nature. 1998; 392:293–296. [PubMed: 9521325]

6. Priori SG, Napolitano C, Gasparini M, Pappone C, Della Bella P, Brignole M, Giordano U, Giovannini T, Menozzi C, Bloise R, Crotti L, Terreni L, Schwartz PJ. Clinical and genetic heterogeneity of right bundle branch block and ST-segment elevation syndrome: a prospective evaluation of 52 families. Circulation. 2000; 102:2509–2515. [PubMed: 11076825]

7. Pfahnl AE, Viswanathan PC, Weiss R, Shang LL, Sanyal S, Shusterman V, Kornblit C, London B, Dudley SC. A sodium channel pore mutation causing Brugada syndrome. Heart Rhythm. 2007; 4:46–53. [PubMed: 17198989]

8. Baroudi G, Pouliot V, Denjoy I, Guicheney P, Shrier A, Chahine M. Novel mechanism for Brugada syndrome: defective surface localization of an SCN5A mutant (R1432G). Circ Res. 2001; 88:E78–E83. [PubMed: 11420310]

9. Kyndt F, Probst V, Potet F, Demolombe S, Chevallier JC, Baro I, Moisan JP, Boisseau P, Schott JJ, Escande D, Le Marec H. Novel SCN5A mutation leading either to isolated cardiac conduction defect or Brugada syndrome in a large French family. Circulation. 2001; 104:3081–3086. [PubMed: 11748104]

10. Valdivia CR, Tester DJ, Rok BA, Porter CB, Munger TM, Jahangir A, Makielski JC, Ackerman MJ. A trafficking defective, Brugada syndrome-causing SCN5A mutation rescued by drugs. Cardiovasc Res. 2004; 62:53–62. [PubMed: 15023552]

11. Brugada R, Brugada J, Antzelevitch C, Kirsch GE, Potenza D, Towbin JA, Brugada P. Sodium channel blockers identify risk for sudden death in patients with ST-segment elevation and right bundle branch block but structurally normal hearts. Circulation. 2000; 101:510–515. [PubMed: 10662748]

12. Antzelevitch C, Pollevick GD, Cordeiro JM, Casis O, Sanguinetti MC, Aizawa Y, Guerchicoff A, Pfeiffer R, Oliva A, Wollnik B, Gelber P, Bonaros EP Jr, Burashnikov E, Wu Y, Sargent JD, Schickel S, Oberheiden R, Bhatia A, Hsu L-F, Haïssaguerre M, Schimpf R, Borggrefe M, Wolpert C. Loss of function mutations in the cardiac calcium channel underlie a new clinical entity characterized by ST-segment elevation, short QT intervals, and sudden cardiac death. Circulation. 2007; 115:442–449. [PubMed: 17224476]

13. Yan GX, Antzelevitch C. Cellular basis for the Brugada syndrome and other mechanisms of arrhythmogenesis associated with ST-segment elevation. Circulation. 1999; 100:1660–1666. [PubMed: 10517739]

14. Weiss R, Barmada MM, Nguyen T, Seibel JS, Cavlovich D, Kornblit CA, Angelilli A, Villanueva F, McNamara DM, London B. Clinical and molecular heterogeneity in the Brugada syndrome: a novel gene locus on chromosome 3. Circulation. 2002; 105:707–713. [PubMed: 11839626]

15. Brisson D, Vohl MC, St-Pierre J, Hudson TJ, Gaudet D. Glycerol: a neglected variable in metabolic processes? Bioessays. 2001; 23:534–542. [PubMed: 11385633]

16. Walz AC, Demel RA, de Kruijff B, Mutzel R. Aerobic sn-glycerol-3-phosphate dehydrogenase from *Escherichia coli* binds to the cytoplasmic membrane through an amphipathic alpha-helix. Biochem J. 2002; 365:471–479. [PubMed: 11955283]

17. Myerburg, RJ.; Castellanos, A. Cardiac arrest and sudden cardiac death. In: Zipes, DP.; Libby, P.; Bonow, RO.; Braunwald, E., editors. Braunwald's Heart Disease: A Textbook of Cardiovascular Medicine. 7th ed.. Philadelphia, Pa: Elsevier Saunders; 2005. p. 865-904.

18. Priori, SG.; Rivolta, I.; Napolitano, C. Genetics of long QT, Brugada, and other channelopathies. In: Zipes, DP.; Jalife, J., editors. Cardiac Electrophysiology: From Cell to Bedside. 4th ed.. Philadelphia, Pa: Saunders; 2004. p. 462-470.

19. Sarkozy A, Brugada P. Sudden cardiac death and inherited arrhythmia syndromes. J Cardiovasc Electrophysiol. 2005; 16:S8–S20. [PubMed: 16138889]

20. Mohler PJ, Schott JJ, Gramolini AO, Dilly KW, Guatimosim S, duBell WH, Song LS, Haurogne K, Kyndt F, Ali ME, Rogers TB, Lederer WJ, Escande D, Le Marec H, Bennett V. Ankyrin-B

mutation causes type 4 long-QT cardiac arrhythmia and sudden cardiac death. Nature. 2003; 21:634–639. [PubMed: 12571597]

21. Schwartz PJ, Priori SG, Dumaine R, Napolitano C, Antzelevitch C, Stramba-Badiale M, Richard TA, Berti MR, Bloise R. A molecular link between the sudden infant death syndrome and the long-QT syndrome. N Engl J Med. 2000; 343:262–267. [PubMed: 10911008]
22. Van Norstrand DW, Valdivia CR, Tester DJ, Ueda K, London B, Makielski JC, Ackerman MJ. Molecular and functional characterization of novel glycerol-3-phosphate dehydrogenase 1–like gene (*GPD1-L*) mutations in sudden infant death syndrome. Circulation. 2007; 116:2253–2259. [PubMed: 17967976]
23. Royer A, van Veen TA, Le Bouter S, Marionneau C, Griol-Charhbili V, Leoni AL, Steenman M, van Rijen HV, Demolombe S, Goddard CA, Richer C, Escoubet B, Jarry-Guichard T, Colledge WH, Gros D, de Bakker JM, Grace AA, Escande D, Charpentier F. Mouse model of SCN5A-linked hereditary Lenegre's disease: age-related conduction slowing and myocardial fibrosis. Circulation. 2005; 111:1738–1746. [PubMed: 15809371]
24. Tan HL, Bink-Boelkens MT, Bezzina CR, Viswanathan PC, Beaufort-Krol GC, van Tintelen PJ, van den Berg MP, Wilde AA, Balser JR. A sodium-channel mutation causes isolated cardiac conduction disease. Nature. 2001; 409:1043–1047. [PubMed: 11234013]
25. Koopmann TT, Beekman L, Alders M, Meregalli PG, Mannens MMAN, Moorman AFM, Wilde AAM, Bezzina CR. Exclusion of multiple candidate genes and large genomic rearrangements in *SCN5A* in a Dutch Brugada syndrome cohort. Heart Rhythm. 2007; 4:752–755. [PubMed: 17556197]
26. Mihm MJ, Yu F, Carnes CA, Reiser PJ, McCarthy PM, Van Wagon DR, Bauer JA. Impaired myofibrillar energetics and oxidative injury during human atrial fibrillation. Circulation. 2001; 104:174–180. [PubMed: 11447082]
27. Fukuda K, Davies SS, Nakajima T, Ong BH, Kupershmidt S, Fessel J, Amarnath V, Anderson ME, Boyden PA, Viswanathan PC, Roberts LJ 2nd, Balser JR. Oxidative mediated lipid peroxidation recapitulates proarrhythmic effects on cardiac sodium channels. Circ Res. 2005; 97:1262–1269. [PubMed: 16284182]
28. Rubart M, Zipes DP. Mechanisms of sudden cardiac death. J Clin Invest. 2005; 115:2305–2315. [PubMed: 16138184]
29. Preliminary report: effect of encainide and flecainide on mortality in a randomized trial of arrhythmia suppression after myocardial infarction: the Cardiac Arrhythmia Suppression Trial (CAST) Investigators. N Engl J Med. 1989; 321:406–412. [PubMed: 2473403]

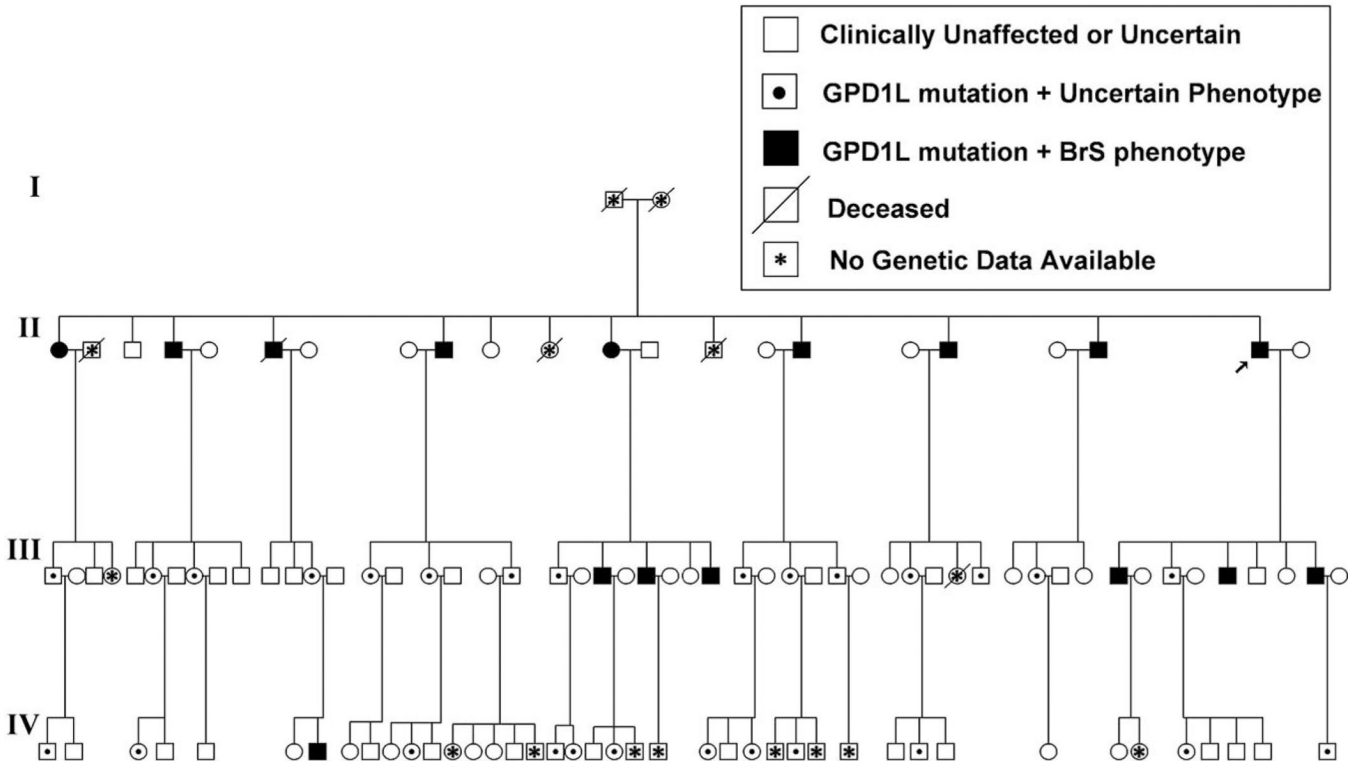

Figure 1.
Pedigree of the FN family. The arrow indicates the proband; squares indicates men; circles, women. Children of genotypically unaffected individuals are not shown. BrS indicates Brugada syndrome.

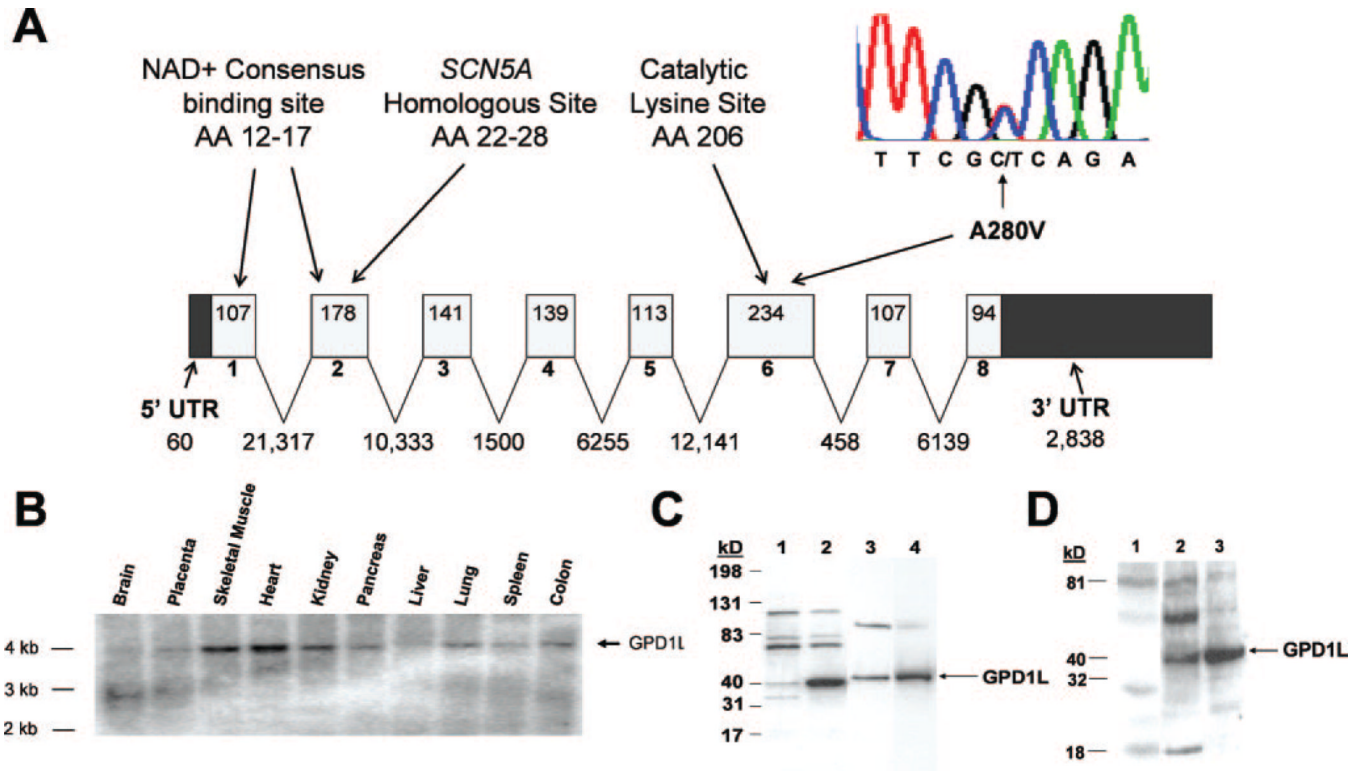

Figure 2.

A mutation in *GPD1-L* causes Brugada syndrome. A, Gene structure of *GPD1-L*. Exons 1 through 8 are indicated by boxes and introns by lines; sizes (bp) are shown inside or below, respectively. Inset, Point mutation (C→T) in exon 6 at amino acid (AA) 280 (A280V) identified in the FN family by DNA sequencing. An area of close homology between amino acids 22 through 28 of GPD1-L and amino acids 830 through 836 in the DIS4-S5 intracellular loop of SCN5A and the area homologous to the putative catalytic site of GPD are noted. B, Expression of GPD1-L RNA. A human multitissue Northern blot (Ambion) was probed with radiolabeled GPD1-L cDNA. C, GPD1-L protein expression by Western blot using a rabbit polyclonal antibody: lane 1, mock-transfected HEK cells; lane 2, HEK cells transfected with human WT GPD1-L; lane 3, total protein from mouse heart; and lane 4, crude membrane fraction from mouse heart. The mouse GPD1-L protein runs slightly larger than human GPD1-L. D, Western blot of GPD1-L in human heart: lane 1, control using preimmune serum; lane 2, total protein from human left ventricle; and lane 3, positive control from COS-7 cells transfected with human WT GPD1-L. Protein (10 μg) was loaded for the HEK/COS-7 cell immunoblots; 20 μg protein was loaded for heart total protein and membrane fraction immunoblots.

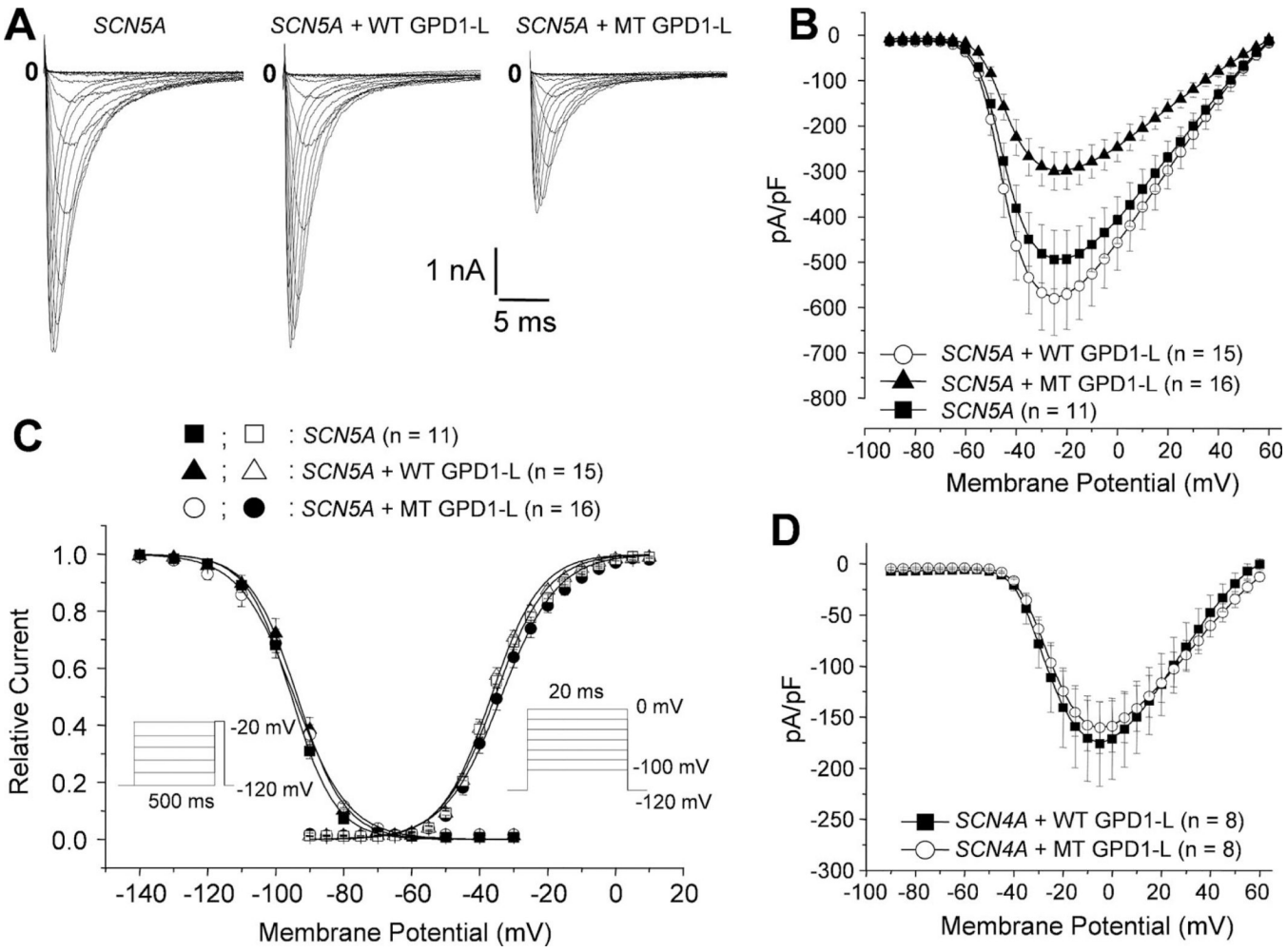

Figure 3.

The A280V GPD1-L mutation decreases I_{Na}. A, Representative currents from an HEK cell line transfected with SCN5A (left) or cotransfected with SCN5A and WT (middle) or A280V GPD1-L (right). Tracings are for 20-ms depolarizations every 5 seconds from a holding potential of −120 to 50 mV in 10-mV steps. The capacitance for each cell is as follows: SCN5A, 8.34 pF; SCN5A+WT GPD1-L, 9.25 pF; and SCN5A+MT GPD1-L, 8.80 pF. B, Current-voltage relationship for peak I_{Na}. Mean cell capacitance for each group is as follows: SCN5A, 7.88±0.47 pF (n=11); SCN5A+WT GPD1-L, 8.61±0.53 pF (n=15); and SCN5A+MT GPD1-L, 8.22±0.40 pF (n=16). C, Steady-state activation and inactivation curves. Inset, Protocols. D, Current-voltage relationship for cells cotransfected with SCN4A and WT vs A280V GPD1-L. MT indicates mock transfected.

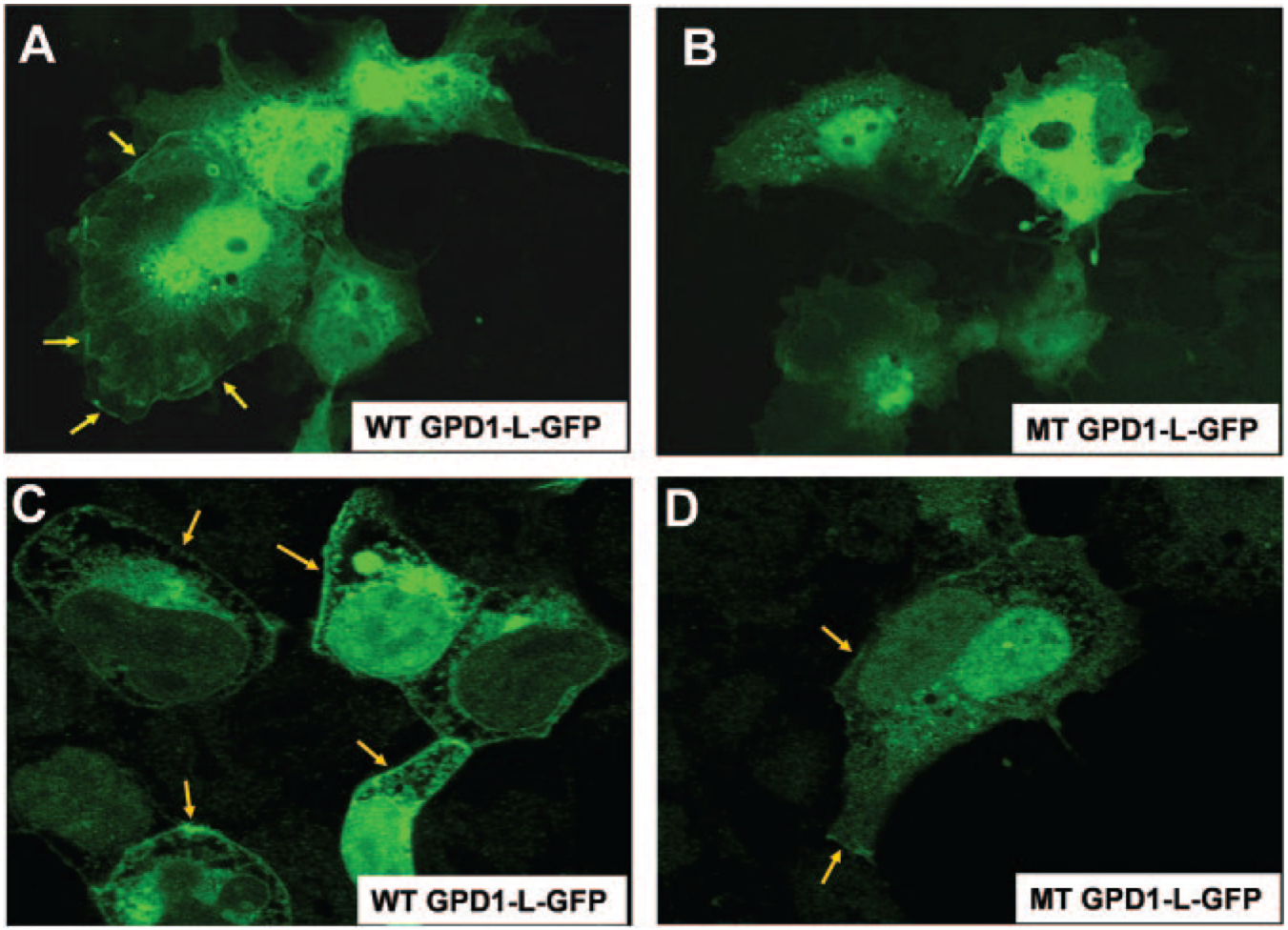

Figure 4.

The A280V mutation reduces localization of GPD1-L adjacent to the cell surface. Confocal fluorescence microscopy of COS-7 cells (A and B) and HEK 293 cells (C and D) transiently transfected with WT GPD1-L–GFP (A and C) or A280V GPD1-L–GFP (B and D). Arrows indicate regions consistent with membrane staining.

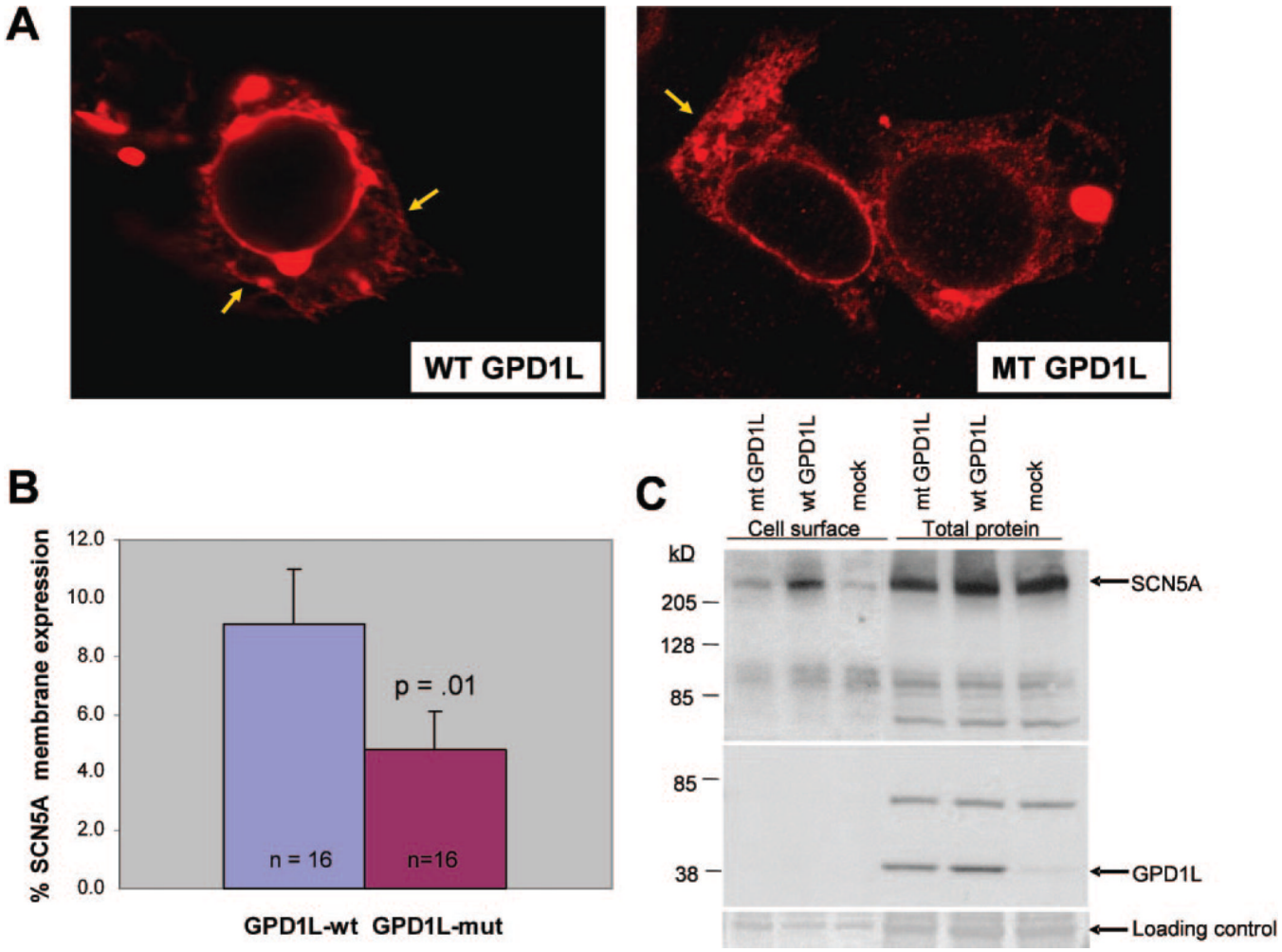

Figure 5.

The GPD1-L mutation decreases SCN5A membrane expression. A, SCN5A immunofluorescence imaged on a confocal microscope of an HEK cell cotransfected with SCN5A and either WT GPD1-L–GFP (left) or A280V GPD1-L–GFP (right). B, Quantification of SCN5A expression near the cell surface in cells cotransfected with SCN5A and WT vs A280V-GPD1-L–GFP (n=16 each). Total cell surface area designated as membrane was not different between the groups (WT, 16.8%; A280V, 16.9%; *P*=NS). No difference existed in total SCN5A protein expression by Western blot (data not shown). C, Surface expression assayed by biotinylation in HEK 293 cells constitutively expressing SCN5A that were mock infected or infected with AAV-WT GPD1-L (WT GPD1L) vs AAV-A280V GPD1-L (MT GPD1-L). Total protein (30 μg) from each group was loaded onto the immunoblot. In this experiment, there was a 45% decrease in cell surface expression of SCN5A, normalized to total protein, in cells infected with AAV-A280V vs WT GPD1-L.